Spectroscopic analysis of Lead Lanthanum Zirconate Titanate Films using UV-VIS and ellipsometry

Running title: a concise title

Sushma Kotru[a,b], Sneha Kothapally[b] and James N. Hilfiker[c]

[a]The University of Alabama, Department of Electrical and Computer Engineering, Tuscaloosa, AL, USA 35487

[b]The University of Alabama, Materials Science Tricampus Program, Tuscaloosa, AL, USA 35487

[c]J.A. Woollam Co., 311 South 7th Street, Lincoln, NE 68508

[a] Electronic mail: skotru@eng.ua.edu

Spectroscopic ellipsometry and Ultraviolet-Visible (UV-VIS) spectrometry were utilized to study the optical properties of ferroelectric lead lanthanum zirconate titanate (PLZT) films. These films were deposited on platinized silicon [Si(100)/ SiO_2/TiO_2/Pt(111)] substrates using the chemical solution deposition method. Films were annealed at two different temperatures (650 and 750ºC) using rapid thermal annealing. Shimadzu UV-1800 UV-VIS spectrophotometer with a resolution of 1 nm was used to measure the reflectance data in the spectral range of 300-1000 nm with a step size of 1 nm. The band gap values were determined from the reflectance spectra using appropriate equations. J.A. Woollam RC2 small spot spectroscopic ellipsometer was used to obtain the change in amplitude *(Ψ)* and phase *(Δ)* of polarized light upon reflection from the film surface. The spectra were recorded in the wavelength range of 210-1500 nm at an incident angle of 65º. Refractive index *(n)* and extinction coefficient *(k)* were obtained by fitting the spectra *(Ψ, Δ)* with the appropriate models. No significant changes were observed in the optical constants of PLZT films annealed at 650 and 750ºC. The optical transparency and the strong absorption in the Ultraviolet (UV) region of PLZT films make them an attractive material for optoelectronic and UV sensing applications.

INTRODUCTION

Lead lanthanum zirconate titanate (PLZT), the most studied ferroelectric material is known to exhibit various properties such as dielectric, pyroelectric, piezoelectric, electro-optic, and photovoltaic in addition to ferroelectric properties.[1,2] Owing to these excellent properties, PLZT has been widely employed in many applications including capacitors,[3] pyroelectric sensors,[4] smart sensors,[5] piezoelectric actuators,[6] microelectromechanical systems,[7] dynamic random access memory,[8] power electronics,[9] and energy storage systems.[10] Due to the optical transparency and electro-

optic effects of PLZT, it has gained interest in optical devices such as photo-actuators,[8] optical shutters,[8] optical modulators,[11] electro-optic deflectors,[12] self-powered UV photodetectors,[13] and integrated nanophotonics.[14]

The optical properties of PLZT are influenced by various factors including the deposition method, type of substrate, annealing temperature and time, annealing environment, and the ratio of lead to lanthanum. Samanta et al. investigated the effect of lead loss on the electrical and optical properties of PLZT ceramics prepared by the sol-gel method. Their studies indicate that sintering at higher temperatures for longer periods of time resulted in greater lead loss, which in turn results in more defects in microstructure and a reduction in the band gap.[15] Jiang et al. observed that the surface morphology of the PLD-grown epitaxial PLZT films, and consequently their optical properties, are influenced by the deposition temperature and oxygen pressures during annealing.[16] Sun et al. utilized the Sol-gel method to prepare PLZT films with varying La content on Si and LNO/Si substrates and investigated the effects of La content on the microstructure, electrical, and optical properties of these films.[17] Nordseth et al. studied the effect of substrate ($SrTiO_3$ and MgO) on the optical properties of sputter deposited PLZT films for optical waveguide applications.[18] Zhang et al. evaluated PLZT films deposited on quartz substrate using PLD for nonlinear optical applications.[19] It is important to note that these studies focused on different compositions of PLZT compared to the one examined in our work.

In this study, the optical properties of $Pb_{0.95}La_{0.05}Zr_{0.54}Ti_{0.46}O_3$ (PLZT) films were measured to evaluate their use as UV sensors. The PLZT films were deposited on Si(100)/ $SiO_2/TiO_2/Pt(111)$ substrate using chemical solution deposition. For this work, PLZT films annealed at two different temperatures (650 and 750ºC) were used. To gather the necessary data, we employed a Shimadzu UV-1800 UV-VIS spectrophotometer for reflectance measurements and a J.A. Woollam RC2 small-spot tool to obtain amplitude *(Ψ)* and phase *(Δ)* spectra of all the films. A comprehensive description of the data acquisition, post-processing techniques, and analytical methods used to extract the optical constants is presented. The data obtained in our study can serve as a valuable reference for other researchers.

SSS Journal Banner

Accession No.:	01892
Optical Property Characterization Technique:	Ultraviolet-Visible (UV-VIS) spectroscopy, Spectroscopic ellipsometry (SE)
Host Material:	Si(100)/ $SiO_2/TiO_2/Pt(111)$ substrate/ $Pb_{0.95}La_{0.05}Zr_{0.54}Ti_{0.46}O_3$/air ambient

Instrument:	UV-Visible Scanning Spectrophotometer (Shimadzu UV-1800), Spectroscopic ellipsometry (J.A. Woollam RC2 small-spot spectroscopic ellipsometer)
Published Spectra:	8
Spectral Category:	Technical

KEYWORDS:

Optical studies, UV-VIS spectroscopy, spectroscopic ellipsometry, reflectance, chemical solution deposition, ferroelectric, PLZT, thin films, annealing temperature, bandgap, refractive index, extinction coefficient, platinized silicon substrate.

SPECIMEN DESCRIPTION

Specimen Number:	01892
Sample Description:	Si(100)/SiO_2/TiO_2/Pt(111) substrate/ $Pb_{0.95}La_{0.05}Zr_{0.54}Ti_{0.46}O_3$/air ambient as depicted in Fig. 1. *the platinum layer was opaque, so it was treated as the "substrate" for optical data analysis
History & Significance	PLZT films possess excellent optical properties, making them highly valuable for a wide range of applications. The combination of optical transparency and electro-optic characteristics makes this material particularly intriguing for optical uses. In this study, PLZT films were prepared on a Si(100)/ SiO_2/TiO_2/Pt(111) substrate by spin-coating the appropriate "Sol". The desired composition of $Pb_{0.95}La_{0.05}Zr_{0.54}Ti_{0.46}O_3$ "Sol" was obtained by dissolving the required amount of solutes in a solvent. The films underwent hydrolysis and pyrolysis after each layer was deposited, repeating the process until the desired thickness was obtained. To enhance crystallinity, the as-deposited films were annealed in a rapid thermal annealing (RTA) furnace at temperatures of 650, and 750ºC. Further information on the preparation of the PLZT solution and thin films, including the processing parameters, can be found in our previous work.[20] The film thickness, measured using a spectroscopic ellipsometer, was determined to be 180 nm. X-ray diffraction analysis revealed that films annealed at 650 and 750ºC

	exhibited a pure perovskite phase without an undesired intermediate pyrochlore phase. The spectral reflectance of the films annealed at 650, and 750ºC were measured using a UV-Visible scanning spectrophotometer. Additionally, a RC2 small-spot spectroscopic ellipsometer was utilized to acquire ellipsometric amplitude *(Ψ)* and phase *(Δ)* spectra from these films
Analyzed Region:	Same as the host material
Sample Conditions During Measurement:	The measurements were conducted at room temperature under normal atmospheric conditions
***Ex Situ* Preparation and Mounting:**	Before mounting the specimens onto the sample stage for measurement, they were carefully blown with dry nitrogen using a blow gun to eliminate any dust. The spot size of the RC2 small-spot ellipsometer was 25 microns by 60 microns, which allowed measurement of a uniform region of the film
***In Situ* Preparation:**	None
FIG. 1. Depiction of specimen layers.	***Ambient:*** air ***Layer 1:*** $Pb_{0.95}La_{0.05}Zr_{0.54}Ti_{0.46}O_3$ film, around 180 nm thickness ***Layer 0 (substrate):*** $Si(100)/SiO_2/TiO_2/Pt(111)$, around 1mm thick *Pt was opaque, so the optical modeling uses this surface as the effective substrate

SPECIMEN COMPONENT LAYERS

■ *Layer 0*

Chemical Name:	Platinized silicon substrate
Layer Composition:	Pt, Ti, Si, O
Structural Formula:	Polycrystalline nature with Pt(111), Si(100)
CAS Registry No:	N/A
Layer Manufacturer/Supplier:	Radiant Technologies, Inc.
As-received Condition:	The 4-inch platinized silicon wafer was divided into smaller pieces measuring 11 mm in length, 11 mm in width, and 1 mm in thickness using a diamond cutter. These smaller pieces, referred to as substrates, were subjected to a series of

	cleaning steps. Firstly, they were ultrasonically cleaned in acetone for 3 minutes, followed by isopropyl alcohol and distilled water. After the cleaning process, the wet substrates were dried by blowing them with dry nitrogen using a blow gun. To prevent moisture absorption, the dried substrates were stored in a desiccator at room temperature
Host Material Characteristics:	Solid, homogeneous, polycrystalline, conductor
Layer Form:	Polycrystalline platinized silicon wafer of dimensions (length:11 mm, width:11 mm, thickness:1 mm)
Lot Number:	N/A
Features Observed:	High conductivity, robustness, improved light absorption, and excellent catalytic activity

■ ***Layer 1***

Chemical Name:	Lead lanthanum zirconate titanate solution prepared using the precursors lead acetate trihydrate, lanthanum acetate, zirconium propoxide, and titanium butoxide
Layer Composition:	$Pb_{0.95}La_{0.05}Zr_{0.54}Ti_{0.46}O_3$
Structural Formula:	Polycrystalline PLZT with tetragonal structure
CAS Registry No:	6080-56-4, 917-70-4, 23519-77-9, and 5593-70-4
Layer Manufacturer/Supplier:	Spin coated PLZT film prepared in house
As-received Condition:	The as-deposited PLZT films were annealed at 650 and 750ºC in a rapid thermal annealing (RTA) furnace. After annealing, the films were stored in a desiccator at room temperature to prevent these films from absorbing the moisture
Host Material Characteristics:	Solid, homogeneous, polycrystalline, dielectric, inorganic compound, thin film
Layer Form:	PLZT film of thickness around 180 nm deposited on a platinized silicon substrate
Lot Number:	N/A
Features Observed:	N/A

INSTRUMENT CONFIGURATION

Instrument #	1 of 2
Instrument Manufacturer:	Shimadzu
Manufacturer Model No:	UV-1800
Instrument Configuration:	Spectrophotometer
Spectral Range:	300-1000 nm
Measurement Angle(s) of Incidence:	5°
Acquired Data Type:	Reflectance vs wavelength

Instrument #	2 of 2
Instrument Manufacturer:	J.A. Woollam
Manufacturer Model No:	RC2 Small-Spot
Instrument Configuration:	Spectroscopic Ellipsometer
Spectral Range:	210-1500 nm
Measurement Angle(s) of Incidence:	65º
Acquired Data Type:	Ψ vs wavelength, Δ vs wavelength

DATA ANALYSIS

To measure the relative specular reflectance in the spectral range of 300-1000 nm, a Shimadzu UV-1800 UV-VIS spectrophotometer with a resolution of 1 nm was utilized. The measurements were conducted at an incident angle of 5º. For this purpose, a specialized sample holder attachment called a specular reflectance attachment was employed. The sample holder consisted of two stages with different diameters and a small aperture: one for the reference (smaller diameter) and the other for the sample (larger diameter). Given the sample size, stages with a 5 mm aperture were selected for this study. To facilitate the measurements, two reflecting mirrors were mounted on the sample and reference stages, with the mirrors facing downwards. Another mirror assembly beneath the sample and reference stages directs the incident light towards the reflecting mirrors. At this stage, the chamber lid was closed, enabling baseline correction within the wavelength range of 300-1000 nm. Subsequently, the reflecting mirror on the sample side was substituted with the sample of interest, and the reflectance mode measurement was conducted.

The reflectance spectra of PLZT films annealed at 650 and 750ºC, as a function of wavelength is presented as Fig. 2.[21] A slight variation in the reflectance values obtained from the films annealed at 650 and 750ºC is due to improved grain size at higher annealing temperatures. There is a drop in the reflectance values around 350 nm corresponding to the strong absorption in ultraviolet (UV) region. The strong absorption in the ultraviolet region makes this material suitable for photovoltaic applications such as UV sensors. The obtained reflectance data was subsequently employed to calculate the band gap of these films using Eqs. (1) and (2), which will be elaborated upon in the Oscillator or effective medium approximation equations..

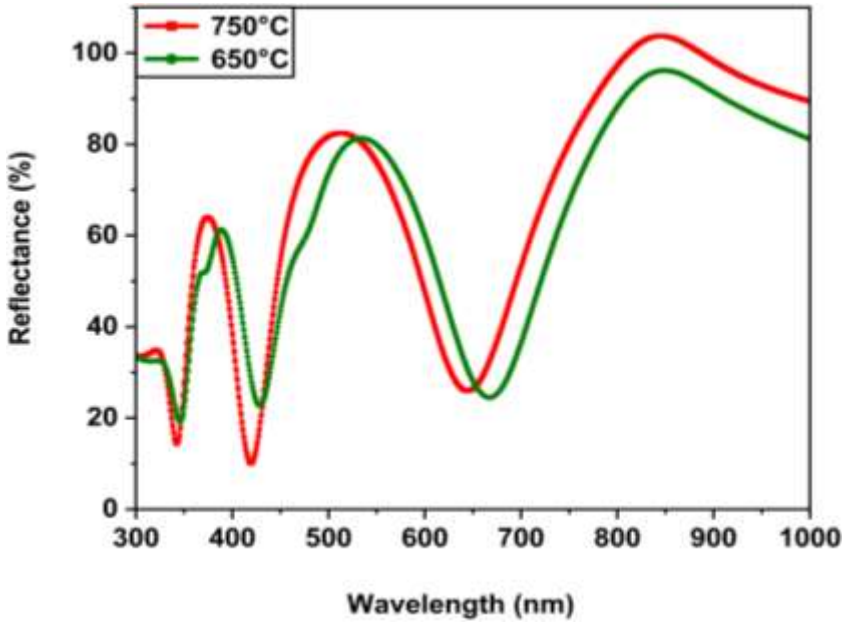

FIG. 2. Reflectance spectra of PLZT films annealed at 650 and 750ºC measured in the wavelength range of 300-1000 nm [Accession No. 01892-01]. Reproduced from Batra *et al*., Opt. Mater. **49**, 123-128 (2015) with permission from the Optical Materials.

To obtain the amplitude ratio *(Ψ)* and phase change *(Δ)* between the parallel and perpendicular components of linearly polarized light upon reflection from the sample surface, a J.A. Woollam RC2 small-spot spectroscopic ellipsometer equipped with CompleteEASE software was utilized. The RC2 uses a dual-rotating compensator optical design with source-fixed polarizer-rotating compensator-sample-rotating compensator-fixed analyzer-detector. Measurements were performed at an incident angle of 65º within the spectral range of 210-1500 nm. The measurement beam size is approximately 25 μm by 60 μm. Before data acquisition, the

hardware was initialized, and the instrument was calibrated using a standard sample (SiO_2/Si wafer, 4 inch in diameter, and oxide thickness approximately 25 nm thick) to align the optics to the sample plane of incidence. The sample of interest was mounted on the sample stage. The stage was adjusted to ensure that the reflected light was centered on the detector. A camera was used to move the measurement site to a uniform region of the thin film. Using the software, the desired parameters to be measured *(Ψ, Δ)* were selected from the data menu. Once the scan was completed, the *(Ψ, Δ)* spectra were obtained and saved on the computer. Figs. 3(a), and 3(b) show the *Ψ* and Δ spectra as a function of wavelength, measured at an incident angle of 65º for the PLZT films annealed at 650, and 750ºC, along with the modeled curves used to match these data.

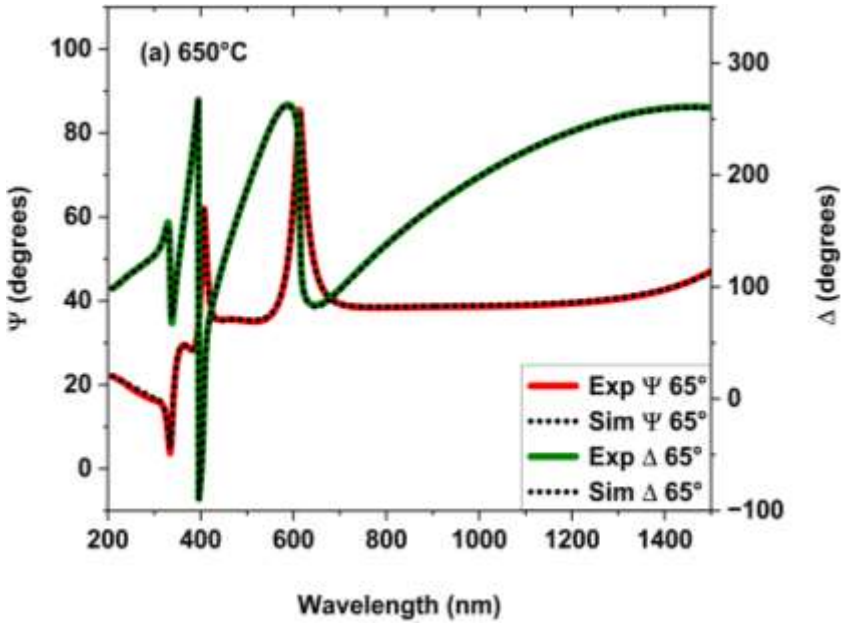

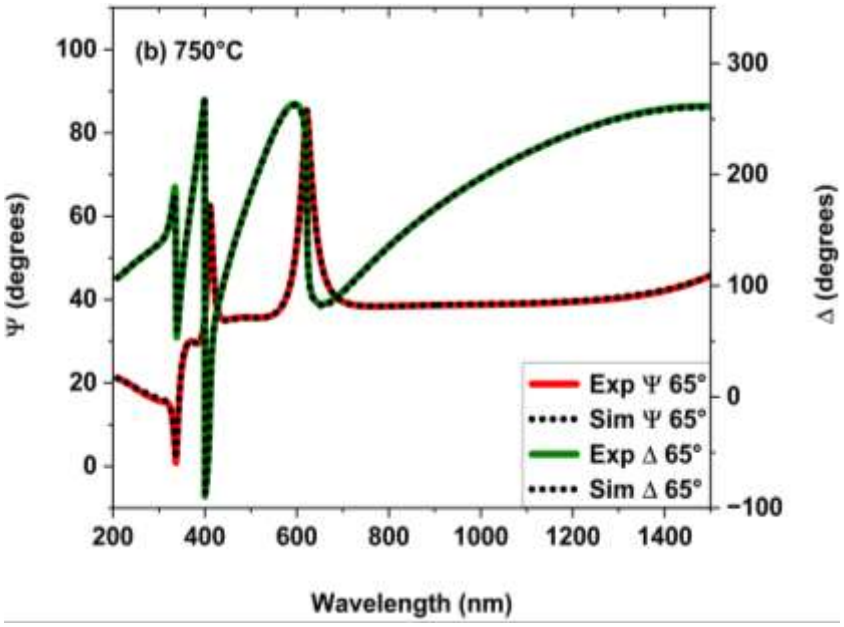

FIG. 3. Ψ and Δ spectra for PLZT films annealed at (a) 650ºC; and (b) 750ºC, measured in the wavelength range of 210-1500 nm at incident angle of 65º along with the corresponding model-fits curves [Accession Nos. (a) 01892-02 and (b) 01892-03].

To obtain the optical parameters including refractive index *(n)* and extinction coefficient *(k)* from the experimental data, an optical model of the structure was constructed using the CompleteEASE® software. This model was designed to simulate the optical measurements, generating simulated data for comparison with the experimental results. Appropriate fitting techniques were employed to obtain the optical constants *(n and k)* with a low mean-squared error.

To construct the desired model, the first layer (layer 0) representing the substrate was initially created, followed by the addition of PLZT layer on top of the substrate. Optical constants for the opaque platinum layer were determined from a direct fit to the bare platinum substrate. The platinum optical constants were modeled using a Kramers-Kronig consistent b-spline layer with no surface layers. These measured values were compared to the optical constants of Platinum from the literature[22] and are presented in Fig. 4. Due to a slight variation between these values, the measured values were fixed in subsequent modeling. The PLZT layer was then

modeled using a summation of three Cody-Lorentz oscillators to describe the absorption features above the bandgap.

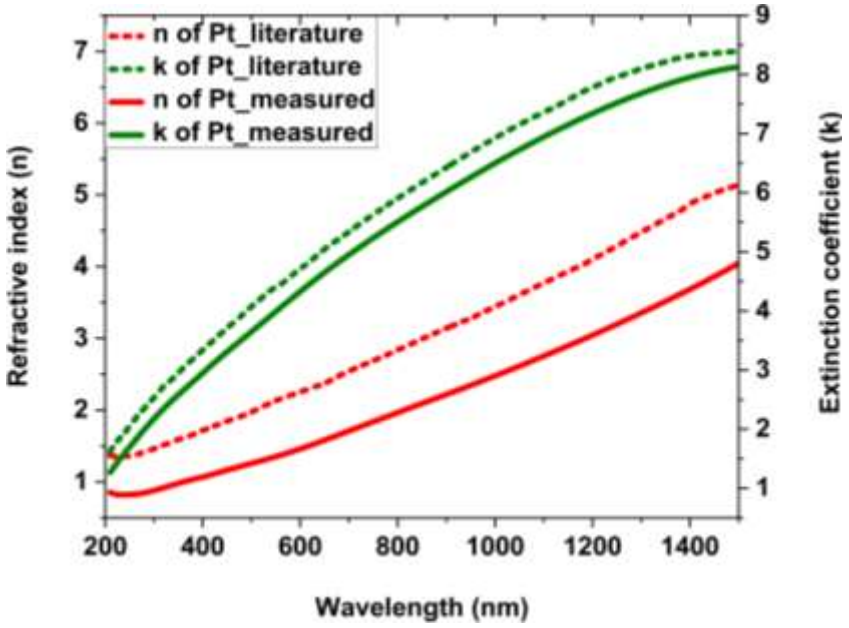

FIG. 4. Measured and literature[22] values of optical constants of platinum as a function of wavelength, where the measured values are from bare substrate [Accession No. 01892-04].

PLZT (1800 Å) films were deposited on Si(100)/SiO_2/TiO_2/Pt(111) substrate, where the thickness of Si, SiO_2, TiO_2 and Pt was 1 mm, 5000 Å, 400 Å and 1500 Å respectively. The platinum layer being thick and thus opaque, it was treated as the substrate and the underlying layers (TiO_2/SiO_2/Si), were not included for optical data analysis. The optical model with two layers used for optical data analysis is presented in Fig. 5. where platinum was modeled as semi-infinite (no light returning from its back surface). A thin surface roughness layer was added to the PLZT layer, which was modeled as a 50%-50% Bruggeman Effective Medium Approximation mixing the underlying PLZT material with void.

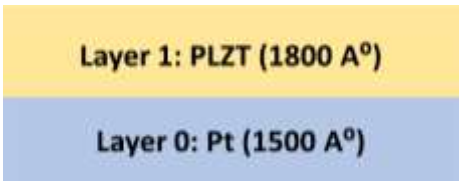

FIG. 5. Schematic of the two-layer optical model used for the optical data analysis.

■ *Oscillator or effective medium approximation equations*

To determine the band gap values of films, the following steps were used. First, the absorption coefficient was calculated from the reflectance data using Kubelka-Munk function [Eq. (1)][23]

$$\alpha = \frac{(1-R)^2}{2R}, \tag{1}$$

where α is an absorption coefficient and R is reflectance.

Next, the absorption coefficient values were employed in the power law of the form [Eq. (2)][23]

$$\alpha h\nu = B\left(h\nu - E_g\right)^n, \tag{2}$$

where $h\nu$ is the incident photon energy, B is the absorption constant, E_g is the band gap, and the value of n depends on if the transition is direct or indirect.

Finally, to obtain the direct band gap values, a plot of $(\alpha h\nu)^2$ versus $(h\nu)$ data was generated. The linear portion of this curve was extrapolated to the photon energy axis $[(\alpha h\nu)^2 = 0]$ to determine the band gap values, as depicted in Fig. 6.[21] The band gap values for the PLZT films annealed at 650, and 750ºC are summarized in Table I. The energy band gap value was 3.536 eV for the film annealed at 750ºC and 3.516 eV for the film annealed at 650ºC, which is not a significant change. These band gap values correspond to the wavelengths in the ultraviolet region.

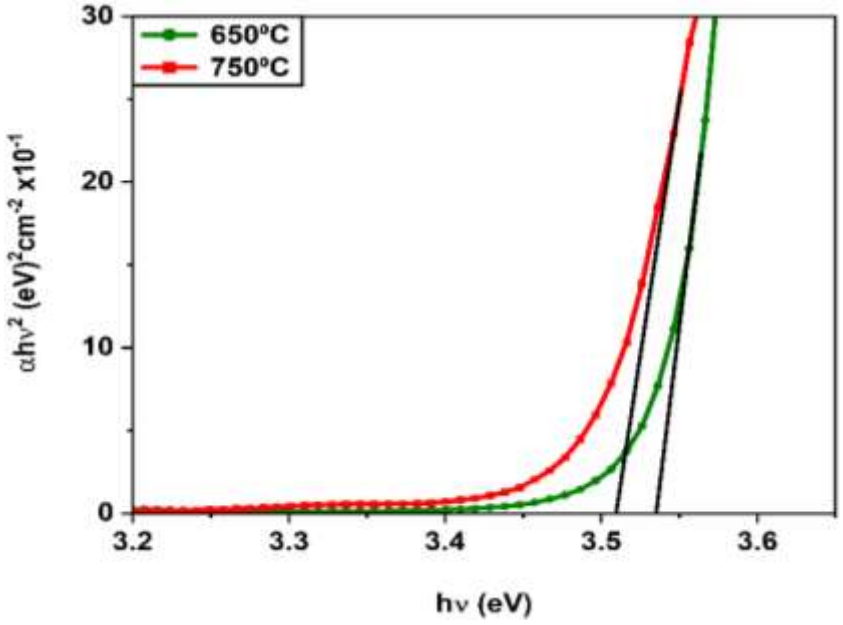

FIG. 6. *(αhν)*^{2} versus *(hν)* plot of PLZT films annealed at 650, and 750ºC [Accession No. 01892-05]. Reproduced from Batra *et al*., Opt. Mater. **49**, 123-128 (2015) with permission from the Optical Materials.

The amplitude ratio *(Ψ)* and the phase difference *(Δ)* of the reflected light are related to each other as per the following equation [Eq. (3)][24]

$$\rho = r_p/r_s = tan(\Psi) * exp^{(i\Delta)}\,, \tag{3}$$

where ρ is the complex reflectance ratio, r_p and r_s are the reflection coefficients of the light polarized parallel and perpendicular to the plane of incidence respectively.

By utilizing the measured parameters *(Ψ, Δ)*, additional information regarding film thickness, refractive index, and extinction coefficient can be extracted. This is achieved by fitting the spectral data *(Ψ, Δ)* with suitable models to establish the best agreement between the experimental and simulated spectra. The optimal fit is determined by minimizing the mean-squared error (MSE). In this work, the Root Mean Squared Error was used to minimize the MSE [Eq. (4)][25]

$$MSE = \sqrt{\frac{1}{3p-m}\sum_{i=1}^{p}\left[\left\{\frac{N_{E_i}-N_{G_i}}{0.001}\right\}^2 + \left\{\frac{C_{E_i}-C_{G_i}}{0.001}\right\}^2 + \left\{\frac{S_{E_i}-S_{G_i}}{0.001}\right\}^2\right]}\,, \tag{4}$$

Where $N = cos(2\Psi)$, $C = sin(2\Psi)cos(\Delta)$, $S = sin(2\Psi)sin(\Delta)$, p represents the number of measured points, m is the number of parameters to be fitted in the optical model, and the parameters subscripted with E and G are the measured and the simulated (model generated) data respectively.

Cody-Lorentz oscillator model without the Urbach absorption was used to fit the measured data to obtain the Cody-Lorentz parameters (A, E_0, C, E_g, E_p) describing the complex dielectric function. The Cody-Lorentz dispersion relations are defined by [Eqs. (5) and (6)][26] with no absorption below the bandgap energy.

$$\varepsilon_2(E) = G(E)L(E) = \left[\frac{(E-E_g)^2}{(E-E_g)^2+E_p^2}\right]\left[\frac{AE_0CE}{(E^2-E_0^2)^2+C^2E^2}\right], \quad (5)$$

$$\varepsilon_1(E) = 1 + \frac{2}{\pi}P\int_{E_g}^{\infty}\frac{E'G(E')L(E')}{E'^2-E^2}dE', \quad (6)$$

where E is the photon energy, ε_1 and ε_2 are the real and imaginary parts of the dielectric constant, $G(E)$ defines the Cody absorption behaviour, $L(E)$ defines the Lorentz oscillator function, A is the absorption amplitude, E_0 is the resonant energy, C is the broadening term, E_g is the bandgap energy, P is the principal part of the integral, and the parameter E_p is used to define the energy, $E_g + E_p$, where the function transitions from a Cody absorption behavior to the Lorentzian absorption. One of the Cody-Lorentz oscillators was at sufficiently high energy to model the contribution from high-energy absorption needed for the Kramers-Kronig integration and negating the need to add any offsets or poles outside the measured spectral range. The contributions from each Cody-Lorentz oscillator were not uniquely defined, leading to correlation between parameters. A different combination of oscillator types could have been used (such as Gaussians, Tauc-Lorentz, etc.), but we preferred to stay with a consistent Cody-Lorentz oscillator, which provided adequate flexibility to describe the overall dielectric function shape. At this point, it is purely curve-fitting to the overall dielectric function and there should not be any physical connection between the oscillator parameters and optical phenomena in the material. The user should note that there is currently no unique sensitivity to the fixed oscillator parameters, but their values provide a good starting point if future measurements are collected to higher photon energies. The final Cody-Lorentz parameters obtained from the optical analysis are tabulated in Table II.

The equation which relates the complex dielectric function *(ε),* and the complex refractive index *(N)* is given by [Eq. (7)][26]

$$\varepsilon = \varepsilon_1 - i\varepsilon_2 = N^2 = (n - ik)^2 \,, \tag{7}$$

where *n* is the refractive index and *k* is the extinction coefficient. The refractive index and extinction coefficient values as a function of wavelength for PLZT films are presented in Figs. 7(a) and 7(b) respectively. From these figures, it is noticed that there is a sharp increase in the refractive index values around 350 nm corresponding to the maximum absorption at these wavelengths. Beyond 350 nm, the extinction coefficient values were observed to be approaching close to 0 corresponding to the low optical losses. These fundamental properties of PLZT films could lead to optoelectronic applications. The optical constants *(n and k)* of PLZT films annealed at 650, and 750ºC are summarized in Table I. From the values listed in Table I, it is clear that there is not a significant change observed in the optical constants of these films with respect to the annealing temperature.

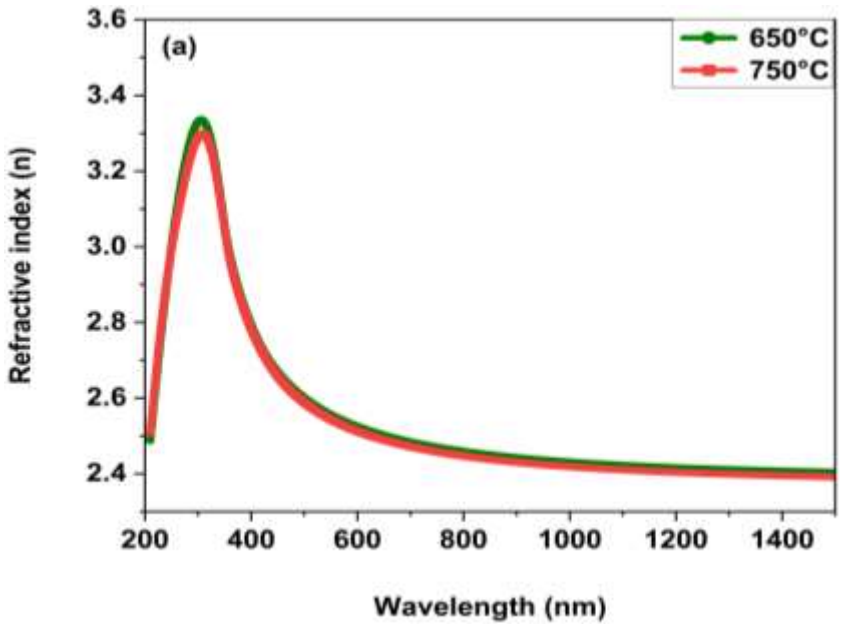

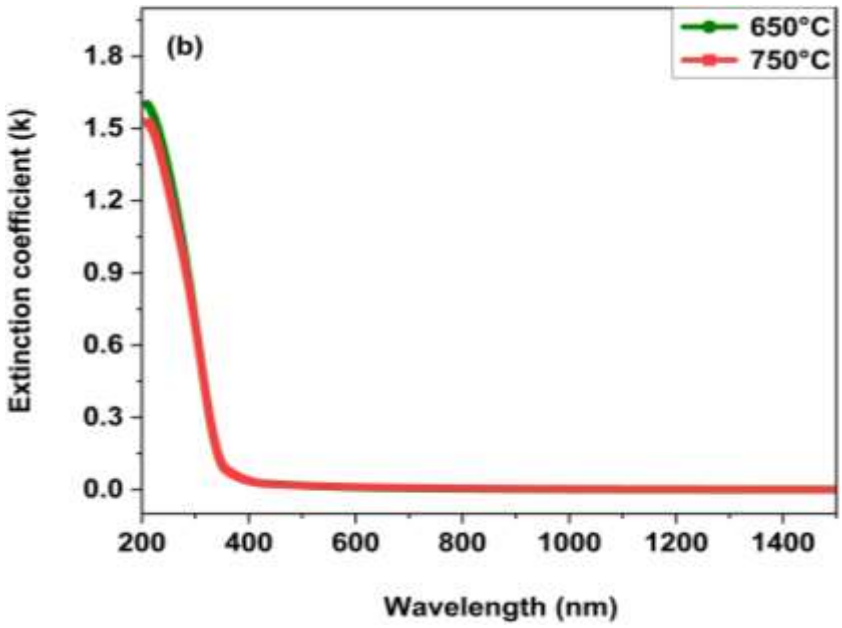

FIG. 7. (a) Refractive index; and (b) Extinction coefficient as a function of wavelength for PLZT films annealed at 650 and 750ºC [Accession Nos. (a) 01892-06 and (b) 01892-07].

Free Parameters in the Model: Band gap, Cody-Lorentz parameters (refractive index, and extinction coefficient), and thickness

Fixed Parameters in the Model: Reflectance, Ψ, Δ, the fixed values of Cody-Lorentz parameters ($\varepsilon_1(\infty)$, C_1, C_2, E_{p_1}, E_{p_2}, E_{p_3}, and E_{g_2}) are given in Table II.

Reference Spectra and Sources: N/A

Table of Structure and Optical Properties

TABLE I. Summary of optical constants of opaque platinum layer and PLZT films annealed at 650, and 750ºC, determined from the UV-VIS reflectance and ellipsometry spectra analysis.

SPECTRAL FEATURES TABLE								
Spectrum ID #	Identity	Composition	Annealing temperature (°C)	Feature or location in Range	Photon Energy (eV)	Wavelength (nm)	n (±0.001)	k (±0.001)
01892-04	Layer 0	Pt	-	-	4.843	256	0.895	1.759
01892-04		Pt	-	-	3.065	405	1.202	2.988
01892-04		Pt	-	-	2.107	589	1.635	4.256
01892-04		Pt	-	-	1.961	633	1.762	4.544
01892-05 01892-06 01892-07	Layer 1	PLZT	650	-	3.536 (Energy band gap)	351	3.046	0.100
01892-06 01892-07		PLZT	650	-	3.065	405	2.777	0.034
01892-06 01892-07		PLZT	650	-	2.107	589	2.531	0.011
01892-06 01892-07		PLZT	650	-	1.961	633	2.509	0.009
01892-05 01892-06 01892-07	Layer 1	PLZT	750	-	3.516 (Energy band gap)	353	3.017	0.094
01892-06 01892-07		PLZT	750	-	3.065	405	2.766	0.034
01892-06 01892-07		PLZT	750	-	2.107	589	2.518	0.013
01892-06 01892-07		PLZT	750	-	1.961	633	2.496	0.011

TABLE II. Thickness, roughness, and Cody-Lorentz parameters obtained from the ellipsometry data analysis of PLZT films annealed at 650, and 750ºC with an MSE of 7.952 and 7.803 respectively.

Sample	Annealing temperature (ºC)	Thickness (nm)	Roughness (nm)	ε_1	ε_2														
					Code-Lorentz Type 1					Code-Lorentz Type 2					Code-Lorentz Type 3				
				$\varepsilon_1(\infty)$	A_1 (eV)	$E0_1$ (eV)	C_1 (eV)	Eg_1 (eV)	Ep_1 (eV)	A_2 (eV)	$E0_2$ (eV)	C_2 (eV)	Eg_2 (eV)	Ep_2 (eV)	A_3 (eV)	$E0_3$ (eV)	C_3 (eV)	Eg_3 (eV)	Ep_3 (eV)
PLZT	650	180.05 ±0.164	8.53 ±0.038	1 (fixed)	9.405 ±0.218	4.014 ±0.015	1 (fixed)	3.457 ±0.008	1 (fixed)	17.965 ±0.142	8.059 ±0.032	1.5 (fixed)	0 (fixed)	2 (fixed)	25.664 ±0.342	5.345 ±0.014	2.319 ±0.033	2.814 ±0.008	2 (fixed)
PLZT	750	182.64 ±0.158	5.42 ±0.036	1 (fixed)	9.414 ±0.195	4.024 ±0.014	1 (fixed)	3.447 ±0.008	1 (fixed)	17.459 ±0.139	7.973 ±0.031	1.5 (fixed)	0 (fixed)	2 (fixed)	26.036 ±0.343	5.387 ±0.014	2.448 ±0.034	2.807 ±0.008	2 (fixed)

ACKNOWLEDGMENTS

This material is based upon work partially supported by the National Science Foundation under Grant No. 1919232. Any opinions, findings and conclusions or recommendations expressed in this material are those of the author(s) and do not necessarily reflect the views of the National Science Foundation. This work utilized resources owned by J. A. Woollam and by the University of Alabama (Electronic Materials and Devices Laboratory).

AUTHOR DECLARATIONS

Conflicts of Interest ***(required)***

The authors have no conflicts to disclose.

Author Contributions ***(if applicable)***

Sushma Kotru: Conceptualization (equal); Data curation (equal); Methodology (equal); Formal analysis (equal); Visualization (equal); Writing – original draft (equal); Writing – review & editing (equal), Project administration (lead); Resources (lead); Supervision (lead); Validation (equal). **Sneha Kothapally:** Conceptualization (equal); Data curation (equal); Methodology (equal); Formal analysis (equal); Validation (equal); Visualization (equal); Writing – original draft (equal); Writing – review & editing (equal). **James Hilfiker:** Methodology (equal); Formal analysis (equal); Writing – review & editing (equal).

DATA AVAILABILITY STATEMENT

The data that supports the findings of this study are available within the article and its supplementary material.

REFERENCES

[1]S. Dutta, R. N. P. Choudhary, P. K. Sinha, and A. K. Thakur, J. Appl. Phys. **96,** 1607-1613 (2004).

[2]M. Qin, K. Yao, and Y. C. Liang, J. Appl. Phys. **105,** 061624 (2009).

[3]M. Wu, Y. Xiao, Y. Liu, H. Li, J. Gao, and L. Zhong, IEEE T. Dielect. El. In. **28,** 6 (2021).

[4]B. B. Bohara, A. K. Batra, and C. R. Bowen, J. Mater. Sci-Mater. El. **29,** 20931-20941 (2018).

[5]R. Singh, A. K. Tripathi, S. Chandra, and T. C. Goel, In Proceedings, 11th International Symposium on Electrets ISE 11, IEEE, pp. 397-400 (2002).

[6]M. D. Nguyen, J. Eur. Ceram. Soc. **39,** 2076-2081 (2019).

[7]H.-J. Zhao, T.-L. Ren, N.-X. Zhang, R.-Z. Zuo, X.-H. Wang, L.-T. Liu, Z.-J. Li, Z.-L. Gui, and L.-T. Li, Mater. Sci. Eng. B **99,** 195-198 (2003).

[8]R. Zachariasz, M. Czerwiec, and J. Ilczuk, Hydroacoustics **8,** 247-254 (2005).

[9]B. Ma, Z. Hu, R. E. Koritala, T. H. Lee, S. E. Dorris, and U. Balachandran, J. Mater. Sci-Mater. El. **26,** 9279-9287 (2015).

[10]H. T. Dang, T. T. Trinh, C. T. Q. Nguyen, T. V. Do, M. D. Nguyen, and H. N. Vu, Mater. Chem. Phys. **234,** 210-216 (2019).

[11]C. Huang, D. Li, T. He, Y. Peng, W. Zhou, Z. Yang, J. Xu, and Q. Wang, ACS Photonics **7,** 3166-3176 (2020).

[12]Q. Ye, Z. Dong, R. Qu, and Z. Fang, In 2007 Conference on Lasers and Electro-optics-Pacific Rim, IEEE, pp. 1-2 (2007).

[13]J. Chen, A. S. Priya, D. You, W. Pei, Q. Zhang, Y. Lu, M. Li, J. Guo, and Y. He, Sensor. Actuat. A-Phys. **315,** 112267 (2020).

[14]J. Xu, C. Huang, J. Dong, W. Zhou, Z. Yang, L. Zhao, Q. Wang, and R. Yang, Opt. Mater. Express **9,** 2279-2290 (2019).

[15]S. Samanta, V. Sankaranarayanan, and K. Sethupathi, J. Mater. Sci-Mater. El. **29,** 7239-7252 (2018).

[16]S. Jiang, C. Huang, H. Gu, S. Liu, S. Zhu, M.-Y. Li, L. Yao, Y. Wu, and G. Zhang, Materials **11,** 525 (2018).

[17]Q. Sun, H. Deng, X. Li, P. Yang, and J. Chu, J. Phys. Conf. Ser. **276,** 012186 (2011).

[18]Ø. Nordseth, T. Tybell, J. K. Grepstad, and A. Røysert, J. Vac. Sci. Technol. A **27,** 548-553 (2009).

[19]W. F. Zhang, Y. B. Huang, and M. S. Zhang, Appl. Surf. Sci. **158,** 185-189 (2000).

[20]V. N. Harshan, and S. Kotru, Integr. Ferroelectr. **130,** 73-83 (2011).

[21]V. Batra, S. Kotru, M. Varagas, and C. V. Ramana, Opt. Mater. **49**, 123-128 (2015).

[22]E. D. Palik, Handbook of Optical Constants of Solids, Academic Press, 333-341 (1985).

[23]H. Lin, C. P. Huang, W. Li, C. Ni, S. I. Shah, Y.-H. Tseng, Appl. Catal. B-Environ. **68,** 1-11 (2006).

[24]M. Prabu, I. B. S. Banu, S. T. Sundari, R. Krishnan, K. N. Prakash, Y. C. Chen, and M. Chavali, J. Nanosci. Nanotechno. **13,** 1-7 (2013).

[25]CompleteEASE Software Manual, J.A. Woollam Company, 3-42 (2020).

[26]J. N. Hilfiker, and T. Tiwald, "Dielectric Function Modeling", in H. Fujiwara and R.W. Collins (eds.) Spectroscopic Ellipsometry for Photovoltaics, Volume 1: Fundamental Principles and Solar Cell Characterization, 141-143 (2018).